

Annual Status Report Submitted to  
NASA HQ  
Code SED-05  
Global Geophysics Program  
Washington DC 20546

for

Grant NAGW-3007:

Analysis of Space Geodetic Measurements for Studying  
the Dynamics of the Solid Earth

Submitted by

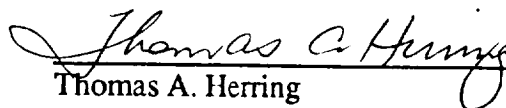
Thomas A. Herring

Department of Earth, Atmospheric, and Planetary Sciences  
Massachusetts Institute of Technology  
Cambridge MA 02139

November 13, 1992

For the period 1/1/92 - 12/31/92

Principal Investigator

  
Thomas A. Herring

(NASA-CR-191215) ANALYSIS OF SPACE  
GEODETIC MEASUREMENTS FOR STUDYING  
THE DYNAMICS OF THE SOLID EARTH  
Annual Status Report, 1 Jan. - 31  
Dec. 1992 (MIT) 19 p

N93-12661

Unclass

G3/46 0128460

**Annual Status Report Submitted to NASA HQ**

for

**Grant NAGW-3007:**

**Analysis of Space Geodetic Measurements for Studying  
the Dynamics of the Solid Earth**

*Short Period Earth Rotation Variations*

We have now completed the analysis of 1085 VLBI experiments, each of approximately 24-hours duration, carried out between January, 1984 and June, 1992. From this analysis we have been able to determine the tidally-coherent components of the diurnal and semidiurnal variations in rotation rate and rotation axis position with accuracies of approximately  $1.5 \mu\text{s}$  for time quantities and  $20 \mu\text{as}$  for the pole position. We attach a paper presented at the COSPAR meeting in Washington in July, 1992 that discusses these results.

*Applications of GPS to monitoring Earth rotation*

We have continued research in this area and worked closely with the Scripps group in setting up the initial GAMIT/GLOBK analysis of the International GPS Service (IGS) campaign data. These data are generating pole position estimates with unprecedented precision, time resolution and duration. We are now carrying out a detailed comparison of VLBI and GPS estimates of pole positions over the July 26, 1992 to August 10, 1992 Epoch 92 campaign interval.

## DIURNAL AND SEMIDIURNAL VARIATIONS IN EARTH ROTATION

T. Herring

Massachusetts Institute of Technology, Cambridge, MA 02139

## ABSTRACT

During the last decade there has been an unprecedented improvement in both the accuracy and the temporal resolution of Earth rotation measurements. Determination of the position of the Earth's rotation axis both in inertial space and with respect to the crust with accuracies of about 0.3 milliarcseconds (mas) are now routine. In recent years, there has been an emphasis on the determination of short-period (daily and less) variations in Earth rotation. Two space based geodetic systems, very long baseline interferometry (VLBI) and the global positioning system (GPS) have proved to be very successful in this endeavor. Results for the tidally coherent part of the subdaily Earth rotation variations determined from the analysis of VLBI data are discussed. The magnitude of other subdaily variations are also considered,

## INTRODUCTION

Variations in the rotation of the Earth are caused by the response of the Earth to external torques from the Sun, Moon and planets; by the response of the Earth to internal mass redistributions from surface and internal loads; and by exchanges of angular momentum between the solid Earth and its fluid elements (ocean, atmosphere and fluid inner core). (See /1/ for a recent review.)

In studies of the rotation of the Earth, two primary coordinates systems are used—one attached in specified manner to the surface of the Earth (the Terrestrial Reference System, TRS) and one attached to inertial space in which equations of motion can be specified (the Celestial Reference System, CRS). Other intermediate coordinate systems are also useful and one attached to the rotation axis of the Earth is commonly used, although care must be taken when using this system to ensure the correct equations of motions are used and that the full transformation between the TRS and CRS is evaluated because invariably the rotation axis moves with respect to both of the systems. In all space geodetic analyses, it is necessary to evaluate the transformation between the TRS and CRS because the observations are made between objects whose coordinates change slowly or not at all in one system but not the other. For example, coordinates of Earth based receivers are slowly changing in the TRS whereas the coordinates of the transmitter (quasars or satellites) are either fixed or expressible in the CRS. To instantaneously transform between the TRS and CRS requires only three rotation angles be known assuming that the origins of the two systems are coincident. Conventionally, however, five angles have been used to express this transformation by introducing an intermediate coordinate system approximately aligned with the rotation axis of the Earth. The advantage of this latter approach has been that, at some level of accuracy, the angular arguments of the rotation matrices change slowly with time. (As we will see this is not the case when rotation variations of less than 1 milliarcsecond (mas) are studied). The conventional transformation between the TRS and CRS is given by:

$$\mathbf{R}_{ti} = \mathbf{PNSW} \quad (1)$$

where  $\mathbf{R}_{ti}$  is the rotation matrix to instantaneously transform between the TRS and the CRS, and  $\mathbf{PNSW}$  is the product of four rotation matrices. The  $\mathbf{W}$  matrix rotates the Z-axis of the TRS to the intermediate axis (called the Celestial Ephemeris Pole, CEP) using the  $X_p$  and  $Y_p$  components of polar motion, the  $\mathbf{S}$  matrix rotates about the Z-axis of the coordinate system by an angle related to the rotation rate of the Earth and conventionally expressed in terms of Greenwich mean sidereal time (GMST) and the (small) difference between this rotation and the instantaneous direction of the Greenwich meridian as expressed by Universal Time; the  $\mathbf{PN}$  matrix finally rotates the coordinate system to one which is fixed in inertial space using the nutation angles and precession. If the Earth's rotation was only affected by external torques whose frequencies when viewed from the TRS were all close to -1 cycles-per-sidereal-day (cpsd) and all other variations in the rotation occurred on time scales long compared to a day then all of the arguments of these rotation matrices would be changing slowly. However, this

is not the case when sub-milliarcsecond rotation variations are considered. Here we will use the conventional formulation as a starting point and express the more complicated rotational motion of the Earth as corrections to the angular arguments of the transformation in Equation (1).

### PARAMETERIZATION

In conventional analyses, the argument of the  $S$  matrix,  $\theta$ , (Greenwich sidereal time), is given by

$$\theta = GMST_{0hr} + R UT1 + \Delta\psi \cos \epsilon \quad (2)$$

where  $GMST_{0hr}$  is Greenwich Mean Sidereal Time at 0 hours UTC,  $R$  is the ratio of sidereal time to universal time;  $UT1$  is Universal time as measured by the rotation of the Earth, and the term  $\Delta\psi \cos \epsilon$  is the equation of equinoxes [2, 3, 4]. Because only three rotation angles are needed to transform between the TRS and CRS, any rotational variations of the Earth can be represented by allowing continuous variations of the arguments  $X_p$ ,  $Y_p$ , and  $UT1$ . In practice, it is not possible to allow instantaneous, arbitrary variations because the space geodetic data depend on other parameters, such as atmospheric delay variations and clock variations, that also need to be estimated. However, by treating Earth rotation parameters as stochastic processes and enforcing some continuity of the values through the magnitude of the process noise variance, it is possible to estimate time varying Earth rotation parameters along with the parameters which need to be estimated (many of which are also stochastic processes [5, 6]). An example of the subdaily variations in Earth parameters obtained in such an analysis is shown in Figure 1. (The other results shown in Figure 1 will be discussed shortly).

Analysis of a large number of VLBI experiments reveals that the subdaily variations in the Earth rotation parameters often appear dominated by diurnal and semidiurnal periodic signals. If this is the case, then the arguments of the  $W$  and  $S$  matrices can be written as

$$UT1 = \overline{UT1} + u_{-1}^c \cos \theta + u_{-1}^s \sin \theta + u_{-2}^c \cos 2\theta + u_{-2}^s \sin 2\theta \quad (3)$$

$$X_p = \overline{X_p} - m_{+1}^c \cos \theta + m_{+1}^s \sin \theta - m_{-2}^c \cos 2\theta - m_{-2}^s \sin 2\theta - m_{+2}^c \cos 2\theta + m_{+2}^s \sin 2\theta \quad (4)$$

$$Y_p = \overline{Y_p} + m_{+1}^c \cos \theta + m_{+1}^s \sin \theta - m_{-2}^c \cos 2\theta + m_{-2}^s \sin 2\theta + m_{+2}^c \cos 2\theta + m_{+2}^s \sin 2\theta \quad (5)$$

where  $\overline{X_p}$ ,  $\overline{Y_p}$  and  $\overline{UT1}$  are the slowly varying parts of the Earth rotation parameters and the coefficients  $u_{-1}^c$ ,  $u_{-1}^s$ ,  $u_{-2}^c$ , and  $u_{-2}^s$  are the cosine and sine components of the diurnal and semidiurnal variations in  $UT1$ ;  $m_{+1}^c$  and  $m_{+1}^s$  are cosine and sine components of the prograde diurnal polar motion variations,  $m_{-2}^c$  and  $m_{-2}^s$  are cosine and sine components of the retrograde semidiurnal polar motion, and  $m_{+2}^c$  and  $m_{+2}^s$  are the cosine and sine components of the prograde semidiurnal polar motion. The retrograde polar motion components have been retained as corrections to the nutation series in our analysis. Although, the coefficients in equations 3–5 are estimated with frequencies of exactly one and two cycles per sidereal day, the frequency range over which the admittance of the estimates is above 90% is very wide for 24 hour sessions of geodetic data and across the tidal bands ( $\pm 0.1$  cpsd about 1 and 2 cpsd) is greater than 98%. Specifically, a coherent signal with frequency  $f$  will alias into these results with frequency  $f - \Omega$  or  $f - 2\Omega$ , depending upon whether  $f$  is in the diurnal or semidiurnal band. In Figure 2, we show estimates of  $u_{-2}^c$  and  $u_{-2}^s$  from the analysis 1085 VLBI experiments conducted between January 1984 and June 1992. Although these estimates look largely like noise, a spectral analysis of the results (Figure 3) reveals that the results shown in Figure 2 are largely consistent with the noise in the estimates and are dominated by three spectral peaks which, to within the frequency resolution of the spectrum ( $3.3 \times 10^{-4}$  cpsd), correspond with the major semidiurnal tides. In Figures 4–8, we show the spectra of all of the diurnal and semidiurnal variations in Earth rotation parameters. In all cases the significant peaks correspond to major tidal lines and their relative amplitudes are approximately consistent with the tide generating forces, although in some cases there are some long period components which do not correspond to tidal lines.

Such affects in Earth rotation were predicted and estimates made of the amplitudes in 1983 [7] for the M2 tide, and by Brosche [8] for three tidal constituents in each of the diurnal and semidiurnal bands. Given that these

variations appear to be tidally coherent, the parameterization of the diurnal and semidiurnal variations can be formulated such that only variations at the tidal frequencies are allowed. We have formulated the tidal arguments in the same fashion as those used for the nutation series with the explicit inclusion of a GST argument to account for the diurnal and semidiurnal variations. (For consistency with previous tidal work we use GST+ $\pi$  as the argument.) A general tide argument is then written as

$$\varphi_i = a_i \ell + b_i \ell' + c_i F + d_i D + e_i \Omega + f_i (\theta + \pi) \quad (6)$$

where  $a_i$ ,  $b_i$ ,  $c_i$ ,  $d_i$ ,  $e_i$ , and  $f_i$  are integer constants which multiply the conventional time dependent arguments of the motions of the Moon and Sun. The diurnal and semidiurnal variations in the rotation of the Earth can then be expressed as

$$\delta UT1 = \sum_{i=1}^N u_i^c \cos \varphi_i + u_i^s \sin \varphi_i \quad (7)$$

$$\delta X_p = \sum_{i=1}^N -m_i^c \cos \varphi_i + m_i^s \sin \varphi_i \quad (8)$$

$$\delta Y_p = \sum_{i=1}^N m_i^c \sin \varphi_i + m_i^s \cos \varphi_i \quad (9)$$

where  $\delta UT1$ ,  $\delta X_p$  and  $\delta Y_p$  are the tidally coherent variations in UT1 and polar motion, the index  $i$  loops over  $N$  terms in both the diurnal and semidiurnal bands and the coefficients are quadrature components of each of the  $N$  tidal lines. (These coefficients should not be confused with the summed amplitudes in each of the tidal bands, equations 3–5).

## RESULTS

To determine the amplitudes of the tidally coherent variations in the Earth's rotation we have analyzed 1085 VLBI experiments, each of approximately 24-hours durations, carried out between January, 1984 and June, 1992. On average, the experiments were separated by a few days and while this does mean that the full spectrum across the diurnal and semidiurnal bands can not be computed, it has little effect on determining the tidally coherent amplitudes because for these the frequencies are known. Within each of the tidal bands (including the prograde bands) we estimated the complex amplitudes at the eleven largest tidal lines except for the retrograde diurnal band where we estimated signals at the fourteen largest lines and at the frequencies corresponding to retrograde free-core nutation. The details of the type of nutational analysis are discussed in /9, 10, 11/. In Tables 1 and 2 we give the values of these tidal contributions at the four major tidal lines in each of the tidal bands. We estimate that the standard deviation of these estimates arising from noise in the analysis of the VLBI data; from quasi-random high frequency variation in atmospheric angular momentum; and errors in the adopted models for the tidal displacements of the sites (solid-earth tides and horizontal and radial ocean loading) to be 1.4–1.8 micro-time-seconds ( $\mu$ s) for the UT1 components and 20 micro-arc-seconds ( $\mu$ as) for the polar motion. These standard deviations correspond to site displacements of 0.6 mm.

## DISCUSSION

The results presented in Table 1 are reasonably consistent with those presented in /12/ with the largest of the differences being attributed to (1) an increase in the duration of the VLBI data analyzed here and the removal of all VLBI experiments for which the rotational parameters could not be determined to better than one milliarcsecond; (2) the new analysis simultaneously estimates all of the coefficients accounting for the correlations, within a day session, between UT1 and polar motion coefficient estimates (the analysis in /12/ estimated the coefficients separately within each band from the time series within that band); and (3) our inclusion in this new analysis of corrections, in global sense, to the tidal displacement model used in the VLBI analysis. The largest of the corrections to the tidal model expressed as the amplitude of the appropriate (unnormalized) spherical harmonic were 1.5 mm radial and 0.3 mm horizontal, in the diurnal band (displacement at 45° latitude of

3.0 and 0.6 mm), and 0.4 mm radial and 0.2 mm horizontal in the semidiurnal band (displacement at  $45^\circ$  latitude of 0.8 and 0.4 mm). This type of correction to the tide model can accommodate global tidal model errors (such as the effects of mantle anelasticity), but can not account for errors in ocean loading models for example. This latter class of tidal model errors is difficult to account for because if all stations are allowed to have arbitrary tidal displacements, then the rotational component becomes undefined. (Any rotation variations could be represented by displacements of the sites.) One way of resolving this singularity is to adopt as the rotational component that which minimizes the tidal displacements at a selected set of sites. (The rotational component would then depend on the selected sites).

For UT1, there are published values of the expected ocean tide contributions (Table 1) and our results are generally smaller than the ocean tide model values. Comparison between the observed rotation variations and ocean tide models will allow global constraints to be placed on ocean tide models and should provide information about some of the ad hoc parameters used in ocean tide modeling (see /8/). Our results agree, with the standard deviations, of the results given in /13/, except at the K1 frequency where /13/ obtain a much larger estimate. Their analysis used a much smaller data set and did not simultaneously estimate polar motion variations and tidal displacements. Sub-daily variations in Earth rotation parameters have also been observed using the GPS /JPL refs/, although at this time these analyses have only used a stochastic approach.

In absolute terms the largest short period Earth rotation variations occur in the retrograde diurnal band because in this band the torques directly affect the rotation of the solid Earth. The response of the Earth in this band also strongly affects the rotational variations through the presence of the fluid core and the elastic and anelastic properties of the mantle (see /9, 10, 11/ for recent discussions). The only reason for tidally coherent torques outside of this band is because of the non-linear response of the oceans and atmosphere to applied torques at these high frequencies.

While the subdaily variations, outside of the retrograde polar motion band, appear dominated by ocean tide effects, other sources of excitation also exist. Part of the M2 UT1 variation arises from libration in the Earth's rotation due to differences between the equatorial moments of inertia ( $1.9 \mu\text{s}$  /16/), and  $5 \mu\text{s}$  of the O1 prograde polar motion also arises from this same source /16/. There is also a contribution across all of these frequency bands from variations in atmospheric angular momentum. To quantitatively assess the magnitude of this contribution to the polar motion variations, we have integrated the polar motion excitations derived from 2 years of the twice-per-day estimates of AAM from National Meteorological Center (NMC) and spectrally analyzed the results. (The polar motion estimates were high-pass filtered with a Gaussian filter with a full-width-half maximum (FWHM) power width of about 60 days). The PSD function obtained from this analysis is shown in Figure 9 with spectra from the VLBI results superimposed. The excitation function included the wind contribution and assumed that the inverted barometer approximation was still valid at these high frequencies. (Assuming a "rigid" ocean increased the power in the high frequency region by approximately 50%.) We may use this spectra to obtain estimates of the atmospheric contributions to high frequency polar motion. Integrating the power in the AAM spectrum for all frequencies corresponding to periods between 1 and 5 days, the AAM results would indicate that the standard of variations in polar motion with periods less than 5 days is  $240 \mu\text{s}$ . This estimate includes the contributions from subdaily variations as well since their power will have been folded into the frequency range -1 to 1 cpsd. If the inverted barometer approximation is invalid at these high frequencies then the power in this frequency range would be  $290 \mu\text{s}$ . (These estimates assume that NMC analysis has not smoothed the excitations excessively. The excitation spectrum show a flattening of spectrum for periods less than 5 days suggesting that any smoothing of the results is probably small, and possibly indicating that much of the excitation may arise from noise in the NMC analysis.) The AAM spectrum can also be used to assess the atmospheric contribution to noise in the estimates of the diurnal and semidiurnal cosine and sine components. The admittance bandwidth for these coefficients is approximately 0.8 cpsd (half power point), and the total variance in a 0.8 cpsd bandwidth about 1 cpsd is  $90 \mu\text{s}$  ( $108 \mu\text{s}$  with no inverted barometer correction), indicating that this much noise could enter into the estimates of the cosine and sine coefficients from a single VLBI experiment. We can not directly assess the contribution in the semidiurnal band, but it could not be larger than that for the diurnal band because of the power folding discussed earlier. This is a non-negligible contribution to the best of the VLBI determinations which have standard deviations as low as  $60 \mu\text{s}$ . It is also similar to the differences between daily estimates and the combined analysis results shown in Figure 1.

## CONCLUSIONS

From the long history of VLBI experiments extremely accurate estimates of the tidally coherent variations of Earth rotation in the diurnal and semidiurnal bands can be determined with the largest uncertainty in these results arising from the potential errors in the tidal displacements models used at the (small number) of VLBI sites. The VLBI results also show that remaining variation after removing the tidal signal is probably less than 300  $\mu$ s (one standard deviation) for pole position and 20  $\mu$ s for UT1. (Because of the wide admittance bandwidth of the estimates of the diurnal and semidiurnal signals, nearly all of the power of signals with frequencies greater than 1-cpsd will be present as the noise level in the VLBI spectra.) However, in the period range between 1 and a few days which is not continuously sampled by VLBI because of the spacing of the experiments, there are likely to be interesting signals related to the oceanic response to atmospheric pressure changes. In addition, the current deployment of global GPS networks provides great promise for resolving more detail in the sub-daily spectral regime although it is not clear currently that the AAM estimates will be accurate enough to allow an interpretation of these results. With several years of data, GPS should also provide robust estimates of the tidally coherent variations as well (except in the retrograde diurnal band) and will have the advantage over VLBI of far greater global distribution of stations.

Acknowledgments: This work was supported by NASA Grant NAGW-0037, NOAA Grant NA90AA-D-AC481, the NSF Grant EAR-89-05560, and by the Kerr-McGee Foundation.

## REFERENCES

1. J. M. Wahr, The Earth's rotation, *Ann. Rev. Earth Planet Sci.*, 16, 231–249, 1988.
2. Woolard, E. W., Theory of the Rotation of the Earth around its center of mass, *Astr. Pap. Amer. Eph. Naut. Almanac XV*, I, pp. 1-165, 1953.
3. Aoki, S., Guinot, B., Kaplan, G.H., Kinoshita, H., McCarthy, D. D., Seidelmann, P. K., "The New Definition of Universal Time," *Astron. Astrophys.*, 105, pp. 359-361, 1982.
4. Aoki, S. and Kinoshita, H., "Note on the relation between the equinox and Guinot's non-rotating origin," *Celes. Mech.*, 29, pp. 335-360, 1983.
5. Herring, T. A., J. L. Davis, and I. I. Shapiro, Geodesy by radio interferometry: The application of Kalman filtering to the analysis of VLBI data, *J. Geophys. Res.*, 95, 12561–12581, 1990.
6. Herring, T. A., and D. Dong, Current and future accuracy of Earth rotation measurements, in *Proceedings of the Chapman conference on Geodetic VLBI: Monitoring Global Change*, NOAA Publication, W. E. Carter (Ed.), 306–324, 1991.
7. Baader, H. -R., P. Brosche, and W. Hovel, Ocean Tides and Periodic Variations of the Earth's Rotation, *J. Geophys.*, 52, 140-142, 1983.
8. Brosche, P., U. Seiler, J. Sündermann, and J. Wunsch, Periodic Changes in Earth's Rotation due to Oceanic Tides, *Astron. Astrophys.*, 220, 318-320, 1989.
9. Mathews, P. M., B. A. Buffet, T. A. Herring, and I. I. Shapiro, Forced nutations of the Earth: Influence of inner core dynamics 1. Theory, *J. Geophys. Res.*, 96, 8219–8243, 1991.
10. Mathews, P. M., B. A. Buffet, T. A. Herring, and I. I. Shapiro, Forced nutations of the Earth: Influence of inner core dynamics 2. Numerical results and comparisons, *J. Geophys. Res.*, 96, 8243–8258, 1991.
11. Herring, T. A., B. A. Buffet, P. M. Mathews, and I. I. Shapiro, Forced nutations of the Earth: Influence of inner core dynamics 3. Very long baseline interferometry data analysis, *J. Geophys. Res.*, 96, 8259–8274, 1991.
12. Herring, T. A., The ZMOA-1990 nutation series, in *Proceedings of IAU colloquium No. 127*, Kulwer Academic Publishers, Dordrecht, Netherlands, 1991.
13. Brosche, P., J. Wunsch, J. Campbell, and H. Schuh, Ocean Tide Effects in Universal Time Detected by VLBI, *Astron. Astrophys.*, 245, 676-682, 1991.
14. Lichten, S. M., S. L. Marcus, and J. O. Dickey, Sub-Daily Resolution of Earth Rotation Variations with Global Positioning System Measurements, *Geophys. Res. Lett.*, in press, 1992a.

15. Lindqwister, U. J., A. P. Freedman, and G. Blewitt, Daily estimates of the Earth's pole position with the Global Positioning System, *Geophys. Res. Lett.*, *19*, 845-848, 1992.
16. Chao, B. F., D. Dong, H. S. Lui, and T. A. Herring, Libration in the Earth's rotation, *Geophys. Res. Lett.*, 2007-2010, 1991.



**TABLE 1.** Observed and Theoretical Amplitudes of the Diurnal and Semidiurnal UT1 Variations.

Fundamental Arguments						Tide	Observed		Brosch§	
$\ell$	$\ell'$	$F$	$D$	$\Omega$	$\theta+\pi$		cos	sin	cos	sin
							( $\mu$ ts)	( $\mu$ ts)	( $\mu$ ts)	( $\mu$ ts)
<u>Diurnal UT1*</u>										
1	0	2	0	2	-1	O1	-17.3	-16.1	-14.2	-36.3
0	0	2	-2	2	-1	P1	-3.9	-5.9	-6.5	-3.6
0	0	0	0	0	-1	K1	6.5	17.8	15.0	12.0
1	0	2	0	2	-1	Q1	-3.1	-4.4		
<u>Semidiurnal UT1†</u>										
1	0	2	0	2	-2	M2	-10.8	14.3	-20.0	26.7
0	0	2	-2	2	-2	S2	-0.1	8.6	-1.2	16.2
0	0	0	0	0	-2	K2	0.8	3.7		
1	0	2	0	2	-2	N2	-1.6	2.8	-4.6	5.9

\* The root mean square (RMS) scatter of the other 14 spectral components estimated is 1.5  $\mu$ ts. We estimate the standard deviations of the terms given to be 1.6  $\mu$ ts

† The RMS scatter of the other 14 spectral components estimated is 0.4  $\mu$ ts. We estimate the standard deviations of the terms given to be 1.4  $\mu$ ts.

§ We have repeated Brosch's calculations accounting for the effects of the fluid core which generally increases the UT1 signals by about 13%.

**TABLE 2.** Observed Amplitudes of the Diurnal and Semidiurnal Polar motion Variations.

Fundamental Arguments						Tide	Retrograde¶		Prograde§	
$\ell$	$\ell'$	$F$	$D$	$\Omega$	$\theta+\pi$		cos	sin	cos	sin
							( $\mu$ as)	( $\mu$ as)	( $\mu$ as)	( $\mu$ as)
<b>Diurnal Polar Motion*</b>										
0	0	2	0	2	-1	O1	-54	-90	-178	89
0	0	2	-2	2	-1	P1	-38	-7	-49	35
0	0	0	0	0	-1	K1			133	-74
1	0	2	0	2	-1	Q1	14	-24	-33	11
<b>Semidiurnal Polar Motion†</b>										
0	0	2	0	2	-2	M2	-10	265	1	-58
0	0	2	-2	2	-2	S2	-67	99	2	-12
0	0	0	0	0	-2	K2	-26	16	39	-5
1	0	2	0	2	-2	N2	-2	11	12	-12

¶ For the retrograde diurnal polar motion terms, the sin values correspond to in-phase nutation amplitude correction and the cosine terms to the out of phase nutation amplitude corrections. The apriori nutation series is ZMOA-1990-2 discussed in /12/.

§ For the prograde terms the signs of all of the fundamental arguments should be reversed.

\* The RMS scatter of the other 18 spectral components estimated in the retrograde diurnal band is 18  $\mu$ as, and for the other 14 components in the prograde diurnal band 13 is  $\mu$ as. We estimate the standard deviations of the terms given to be 20  $\mu$ as.

† The RMS scatter of the other 14 spectral components estimated in the retrograde semidiurnal band is 8  $\mu$ as, and in the prograde semidiurnal band is 8 is  $\mu$ as. We estimate the standard deviations of the terms given to be 20  $\mu$ as.

Fig. 1. Subdaily variations in Earth rotation parameters obtained from the analysis of three VLBI experiments conducted the National Aeronautics and Space Administration (NASA) as part of the VLBI research and development program. In each of the panels, the dots with simple error bars are the results obtained by estimating (a)  $X_p$ , (b)  $Y_p$ , and (c)  $UT1$  once-per-hour with the estimates treated as a random walk process with a process noise set such that adjacent values were constrained with standard deviation of 0.6 mas for  $X_p$ ,  $Y_p$ , and 0.07 mts for  $UT1$ . The solid line shows the time variation predicted when the amplitudes of diurnal and semidiurnal variations are estimated instead of allowing stochastic variations. One standard deviation errors are shown occasionally on these results. The dashed line shows the variations predicted by the tidally coherent model, given in Tables 1 and 2.

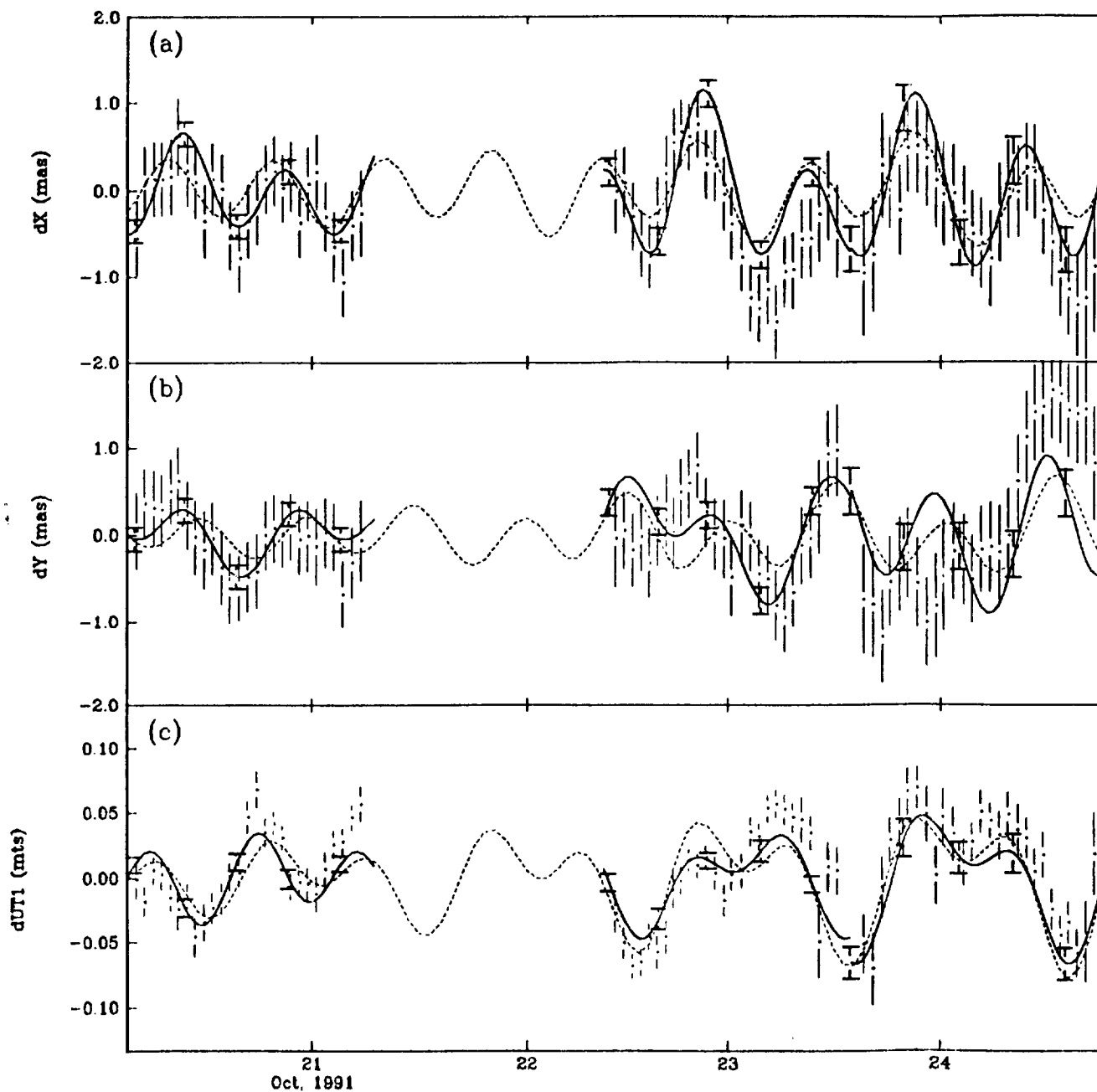


Fig. 2. Estimates of cosine and sine components of the semidiurnal variations in UT1 from the analysis discussed in the text. One standard deviation error bars are shown.

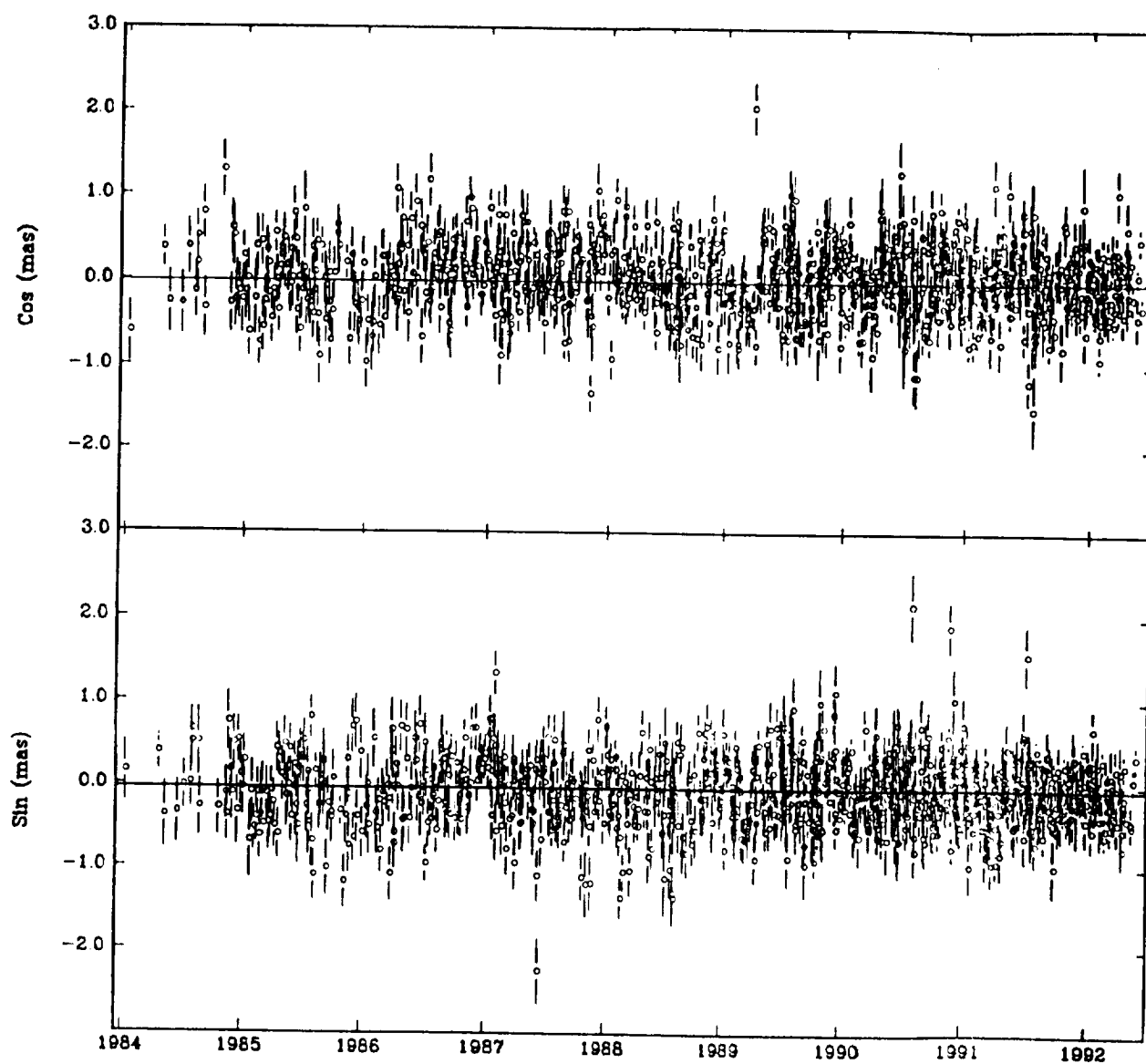


Fig. 3. Log of the Power-spectral density (PSD) function as a function of frequency for the semidiurnal UT1 results shown in Figure 2. The thick (almost horizontal) line is the 99.5% confidence limit computed by propagating the variances in the data estimates through the weak smoother (Gaussian filter with full-width-at-half-maximum of 4 days) used to generate a uniformly spaced data set and through the fast Fourier transform used to generate the PSD. The correlations between the "smoothed" data were accounted for in computing the confidence interval. The spectral resolution is 1/3065 cpsd. For the UT1 spectra, we have expressed the UT1 variations in angular arguments so that Figures 3 and 4 can be directly compared to Figures 5-8.

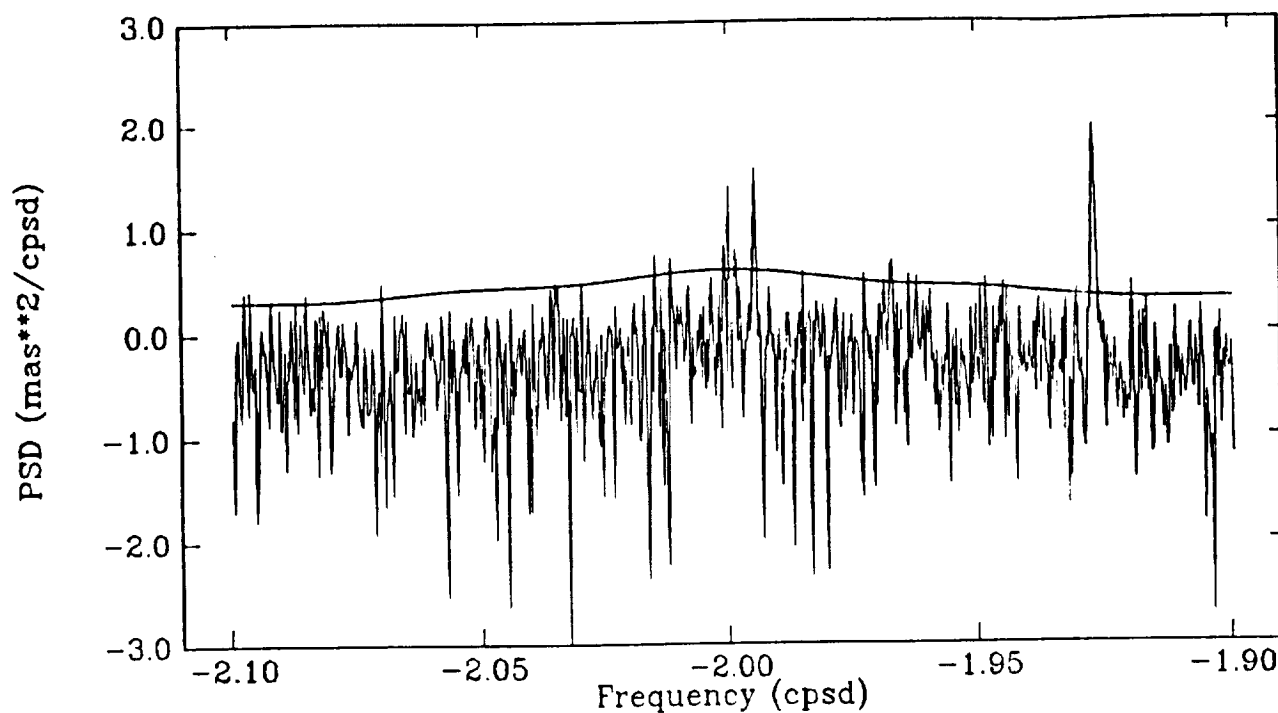


Fig. 4. PSD function of the diurnal UT1 variations (see Fig. 3. for details).

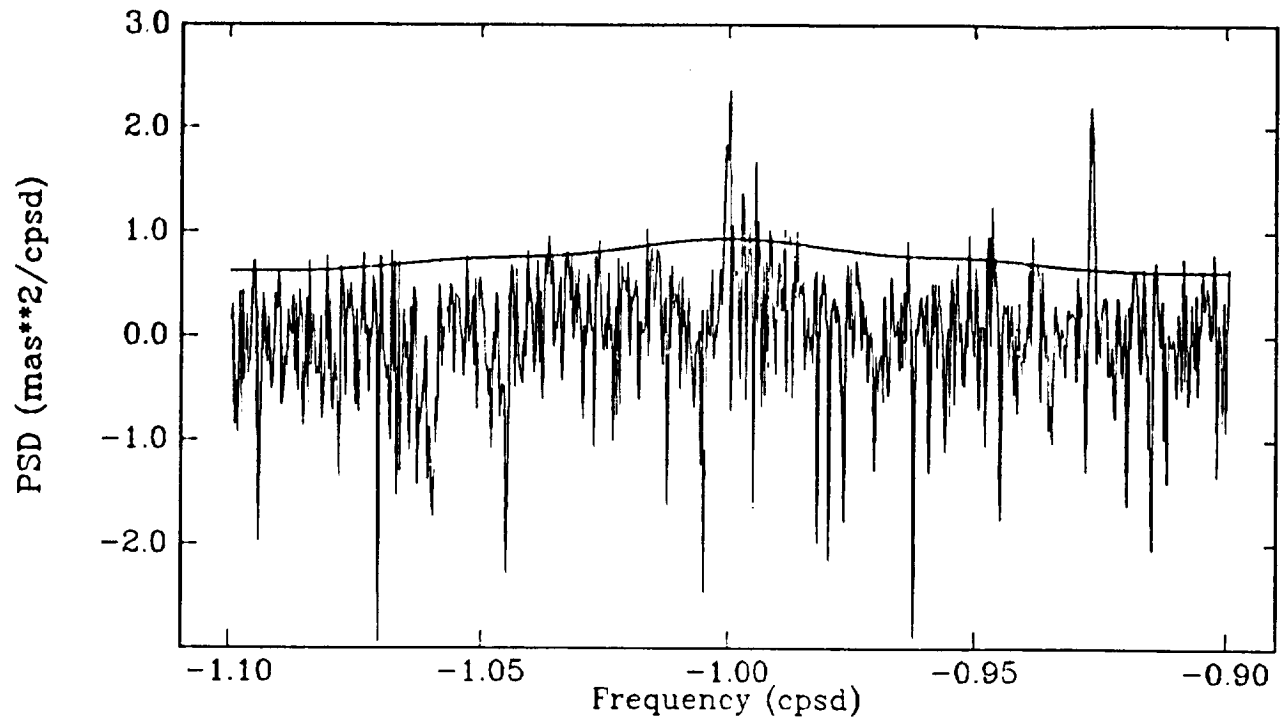


Fig. 5. PSD function of the retrograde semidiurnal polar motion results (see Fig. 3. for details).

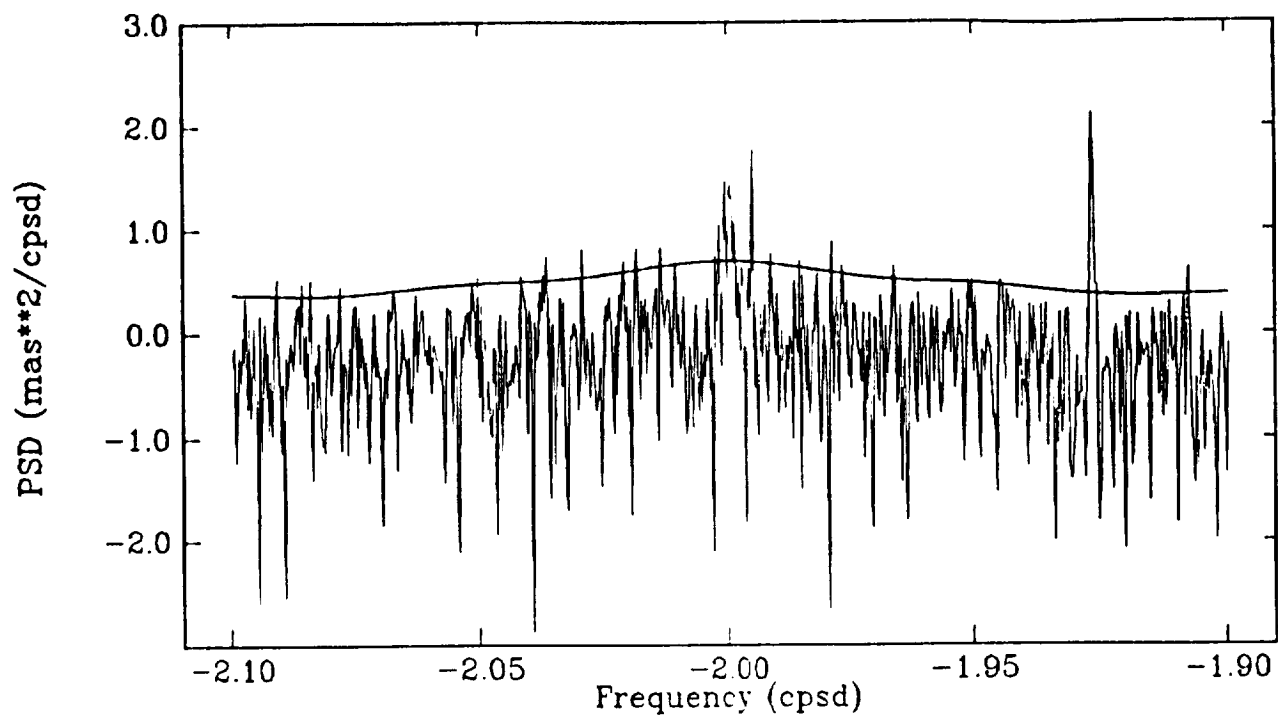


Fig 6. PSD function of the retrograde diurnal polar motion results (see Fig. 3. for details). These results are computed from nutation angle corrections to the ZMOA-1990-2 nutation series.

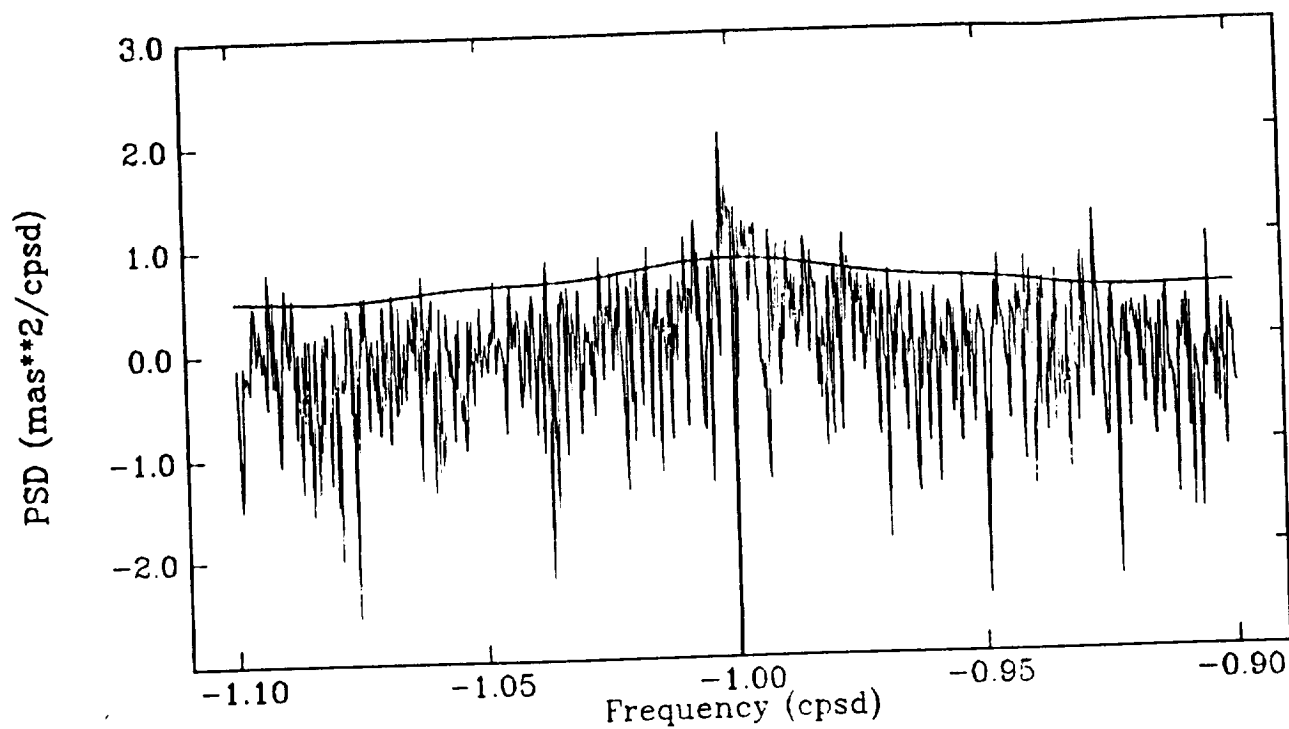




Fig. 7. PSD function of the prograde diurnal polar motion results (see Fig. 3. for details).

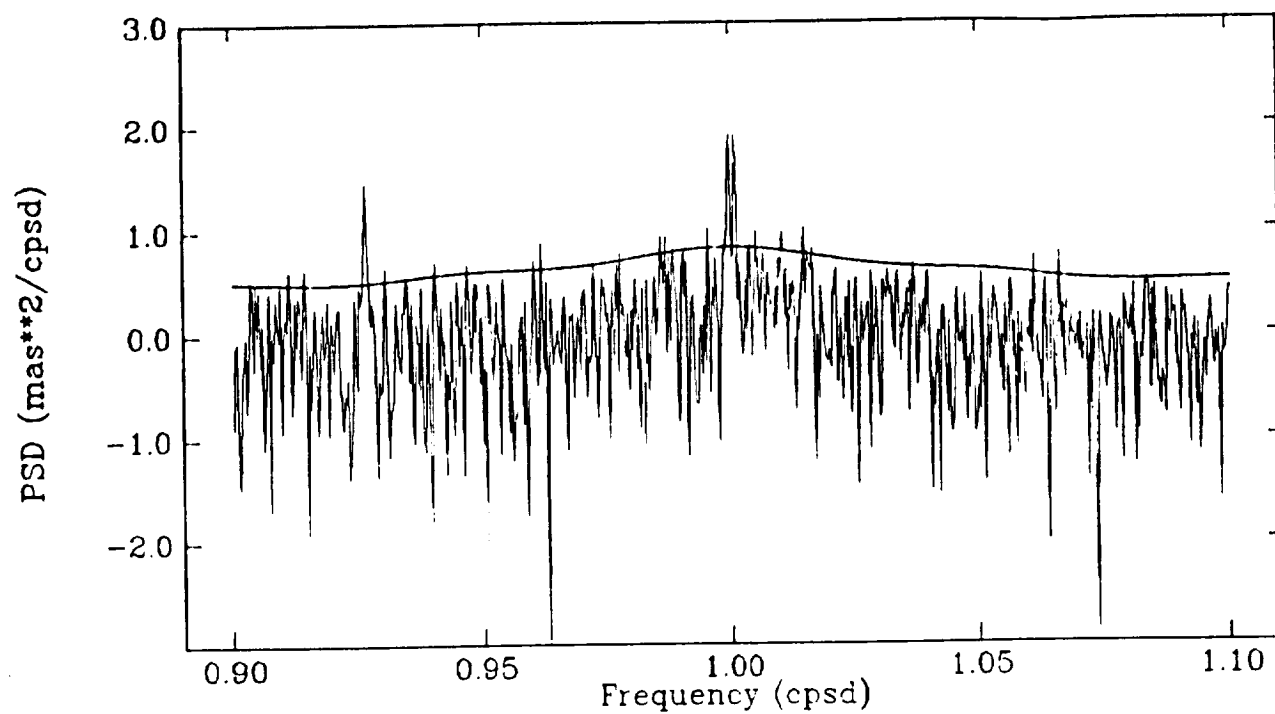


Fig 8. PSD function of the prograde semidiurnal polar motion results (see Fig. 3. for details).

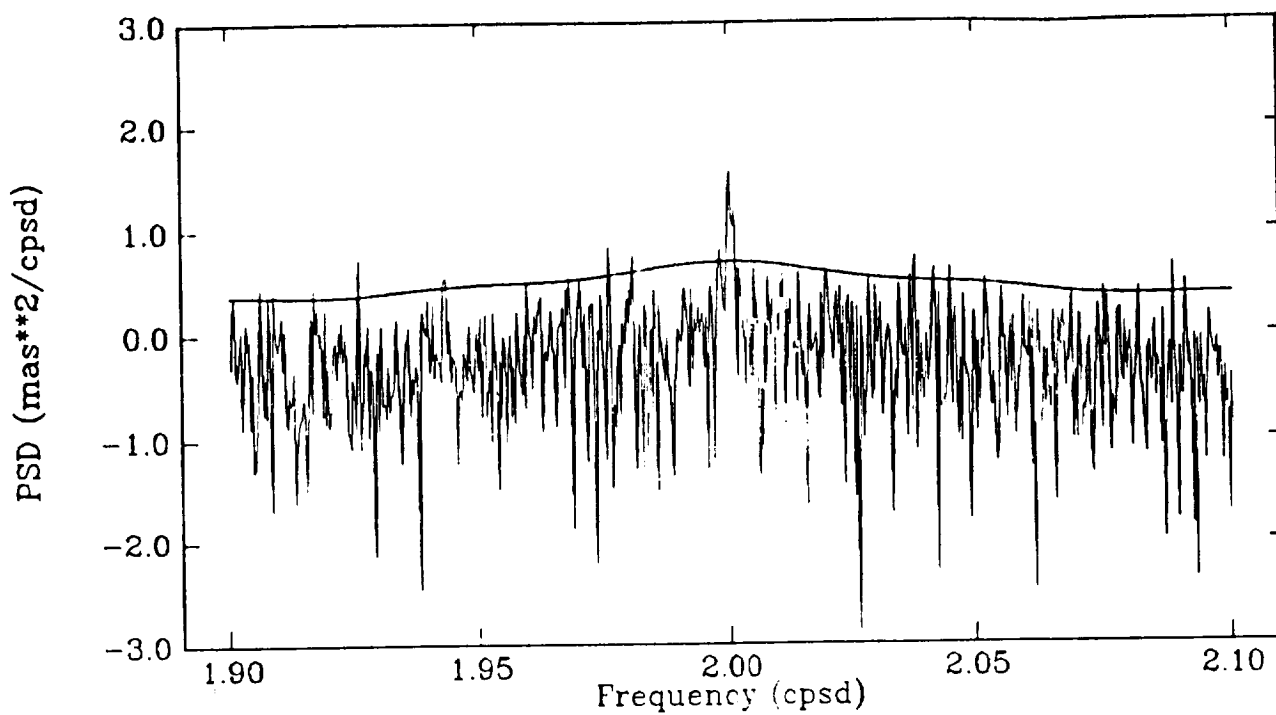


Fig. 9. Composite PSD function of polar motions variations for the frequency range from -2 to +2 cpsd. The dashed line is the PSD of the high-passed filtered AAM polar motion results. (Spectral resolution 1/814 cpsd). The solid lines are the spectra from Figures 6-8. Because of the admittance of a wide spectral bandwidth into the VLBI spectra, the noise power in the VLBI spectra will be four times larger than the AAM i.e., the noise from a 0.8 cpsd bandwidth is compressed into a 0.2 cpsd bandwidth in the VLBI spectra.

